Phenothiazine-triphenylamine based organic dyes containing various conjugated linkers for efficient dye-sensitized solar cells

ARTICLE *in* JOURNAL OF MATERIALS CHEMISTRY · DECEMBER 2012

Impact Factor: 7.44 · DOI: 10.1039/C2JM34682F

6 AUTHORS, INCLUDING:

Zhongquan Wan
University of Electronic Science and Techn…
26 PUBLICATIONS **283** CITATIONS
SEE PROFILE

Yandong Duan
Chinese Academy of Sciences
39 PUBLICATIONS **605** CITATIONS
SEE PROFILE

Yuan Lin
Chinese Academy of Sciences
193 PUBLICATIONS **2,154** CITATIONS
SEE PROFILE

Journal of Materials Chemistry

Cite this: J. Mater. Chem., 2012, 22, 25140

www.rsc.org/materials

PAPER

Phenothiazine–triphenylamine based organic dyes containing various conjugated linkers for efficient dye-sensitized solar cells

Zhongquan Wan,[a] Chunyang Jia,*[a] Yandong Duan,[b] Linlei Zhou,[a] Yuan Lin*[b] and Yu Shi[a]

Received 17th July 2012, Accepted 27th September 2012
DOI: 10.1039/c2jm34682f

In order to increase the electron-donating ability of the donor part of the organic dye, two phenothiazine groups, as additional electron donors, were introduced into a triphenylamine unit to form a starburst donor–donor (2D) structure in this paper. Three new organic dyes (**WD-6**, **WD-7** and **WD-8**) containing this starburst 2D structure and a 2-cyanoacetic acid acceptor linked by various conjugated linkers (benzene, thiophene, and furan) have been designed, synthesized and applied in dye-sensitized solar cells (DSSCs). The introduction of a phenothiazine group with a butterfly conformation in the triphenylamine donor parts has a good influence on preventing the molecular π–π aggregation due to the starburst 2D structure of the organic dye. The conjugated linker effects on the photophysical, electrochemical and photovoltaic properties of these organic dyes were investigated in detail. The DSSCs made with these organic dyes displayed remarkable overall conversion efficiencies, ranging from 4.90–6.79% under an AM 1.5 solar condition (100 mW cm^{-2}). The best performance was found for organic dye **WD-8**, in which a furan group was the conjugated linker. It displayed a short-circuit current (J_{sc}) of 14.43 mA cm^{-2}, an open-circuit voltage (V_{oc}) of 682 mV, and a fill factor (ff) of 0.69, corresponding to an overall conversion efficiency of 6.79%. The different photovoltaic behaviors of the solar cells based on these organic dyes were further elucidated by the electrochemical impedance spectroscopy.

Introduction

Dye-sensitized solar cells (DSSCs), developed by Grätzel and O'Regan, have attracted the considerable attention of many research groups in the past two decades owing to their high efficiency and low cost.[1] DSSCs typically contain four components: a mesoporous semiconductor metal oxide film, a dye, an electrolyte/hole transporter, and a counter electrode.[2] In these components, the dye is a crucial element, exerting significant influence on the conversion efficiency as well as the stability of the cells.

DSSCs based on ruthenium dyes have shown very impressive solar-to-electric power conversion efficiency. Recently, a new record efficiency (11.4%) of a solar cell based on black dye with donor–acceptor type coadsorbent was obtained.[3] However, the large-scale application of ruthenium dyes is limited because of costs and environmental issues. Porphyrin derivatives are the archetypal light collectors of photosynthetic organisms and they are naturally becoming the main focus of the design of new dyes for DSSCs. Indeed, Diau and co-workers have developed very efficient push–pull porphyrin dyes, affording a record efficiency of 10.17% with an I_3^-/I^--based electrolyte,[4] and more recently a 12.3% efficiency for a cobalt electrolyte,[5] which are the best performing sensitizers reported so far. However, the synthetic approach of porphyrin dyes is complicated and the yield is low.

For the above reasons, a lot of effort has been dedicated to the development of pure organic dyes which exhibit not only higher molar extinction coefficients, but also simple preparation and purification at lower cost. Coumarin,[6] squaraine,[7] indoline,[8] phenothiazine,[9] triphenylamine,[10] fluorene,[11] carbazole[12] and tetrahydroquinoline[13] based organic dyes have been developed and show good performance.

Most organic dyes are composed of electron donor, π linker and acceptor moieties and usually have a rod-like configuration. However, the rod-like molecules are elongated, which may facilitate the recombination of electrons with the triiodide and the formation of aggregates between molecules.[14] Therefore, organic dyes with a starburst conformation were designed and synthesized by introducing an additional electron donor group into the D–π–A molecule to form the starburst 2D–π–A structure,[15] which avoids the charge recombination process of injected electrons with the triiodide in the electrolyte and the formation of aggregates between dye molecules.

[a]*State Key Laboratory of Electronic Thin Films and Integrated Devices, School of Microelectronics and Solid-State Electronics, University of Electronic Science and Technology of China, Chengdu 610054, P. R. China. E-mail: cyjia@ uestc.edu.cn; Fax: +86 28 83202569; Tel: +86 28 83201991*
[b]*CAS Key Laboratory of Photochemistry, Institute of Chemistry, BNLMS, Chinese Academy of Sciences, Beijing 100190, P. R. China. E-mail: linyuan@iccas.ac.cn; Fax: +86 10 8261 7315; Tel: +86 10 8261 5031*

Recently, we reported a novel organic dye **WD-1** with a starburst 2D–π–A configuration, in which two phenothiazine groups are introduced into a triphenylamine donor as additional electron donors, and 2-cyanoacetic acid is used as an acceptor.[16] The solar cell based on **WD-1** afforded an overall conversion efficiency of 4.54%, which is higher than that of the corresponding triphenylamine dye. The study suggested that optimizing the triphenylamine donor part by introducing phenothiazine groups as additional electron donors to form a starburst 2D–π–A organic dye is a promising way for preventing unfavorable dye aggregation and increasing the power conversion efficiency.

The linker group between the electron donor and the acceptor in organic dyes plays an important role in terms of optical absorption and charge transfer properties, so this work studies the effect of different linkers on phenothiazine–triphenylamine based starburst 2D–π–A organic dyes. We therefore designed and synthesized three new starburst 2D–π–A organic dyes (**WD-6**, **WD-7** and **WD-8**) with different conjugated linker groups (Scheme 1). These organic dyes comprise phenothiazine–triphenylamine as a starburst electron donor, 2-cyanoacetic acid as an electron acceptor, and the different aromatic groups as a conjugated linker, *i.e.*, benzene, furan, and thiophene. They were successfully applied in DSSCs. The effects of the different conjugated linkers on the photophysical, electrochemical and photovoltaic properties of these organic dyes were investigated in detail.

Experimental

Equipment

NMR spectra were obtained with a Brücker AM 400 spectrometer (relative to TMS). Mass spectra were recorded with a Waters LCT Premier XE spectrometer. The absorption spectra of the dyes in solution and adsorbed on TiO_2 films were measured with a SHIMADZU (model UV2450) UV-vis spectrophotometer. The cyclic voltammograms of the dyes were obtained with a CH Instruments 660C electrochemical workstation using a normal three-electrode cell with a Pt working electrode, a Pt wire counter electrode, and a Ag/AgCl reference electrode.

Materials

Phenothiazine and triphenylamine were purchased from Astatech. 4-Formylphenylboronic acid, 5-formyl-2-thiopheneboronic acid, and 5-formyl-2-furanboronic acid were purchased from J & K Scientific Ltd. Lithium iodide (LiI) was purchased from Acros. 2-Cyanoacetic acid, 4-*tert*-butylpyridine (TBP) and 3-methoxypropionitrile (MPN) were purchased from Aldrich. 3-Hexyl-1-methylimidazolium iodide (HMII) was prepared according to the literature.[17] THF was pre-dried over 4 Å molecular sieves and distilled under an argon atmosphere from sodium benzophenone ketyl immediately prior to use. The starting material, tris(4-iodophenyl)amine, was synthesized according to the corresponding literature method.[14] All other solvents and chemicals were purchased from Aldrich and used as received without further purification.

Preparation of DSSCs

The TiO_2 colloid for liquid-state DSSCs was prepared according to the literature.[18] The FTO glass substrates were immersed in 40 mM $TiCl_4$ aq. at 70 °C for 30 min and washed with water and ethanol. The 12 μm thick mesoporous nano-TiO_2 films, composed of 15–20 nm anatase TiO_2 particles, were coated on the FTO glass plates by doctor blade. After drying the nanocrystalline TiO_2 layer at 125 °C, a 4 μm thick second layer of 300–500 nm sized light scattering anatase particles (Shanghai Cai Yu Nano Technology Co., Ltd) was deposited using a doctor blade onto the first layer. The TiO_2 electrodes were heated at 450 °C for 30 min. After sintering, when the temperature cooled to about 90 °C, the electrodes were immersed in a dye bath containing 0.5 mM **N3** in ethanol or 0.2 mM **WD** dyes in acetonitrile and left overnight. The films were then rinsed in ethanol to remove excess dye. Solar cells were assembled, using a 25 μm thick thermoplastic Surlyn frame, with a platinized counter electrode. An electrolyte solution was then introduced through the hole predrilled in the counter electrode, and the cell was sealed with thermoplastic Surlyn covers and a glass coverslip. The liquid electrolyte employed was a solution of 0.3 M HMII, 0.5 M LiI, 0.05 M I_2 and 0.5 M TBP in MPN.

Photovoltaic characterization

The irradiation source for the photocurrent-density–voltage (*J–V*) measurement is an AM 1.5 solar simulator (91160A, Newport Co., USA). The incident light intensity was 100 mW cm^{-2} calibrated with a standard Si solar cell. The tested solar cells were masked to a working area of 0.2 cm^2. Volt–current characteristics were performed on a Model 2611 sourcemeter (Keithley Instruments, Inc., USA). A Keithley 2611 sourcemeter and a Model spectrapro 300i monochromator (Acton research, USA)

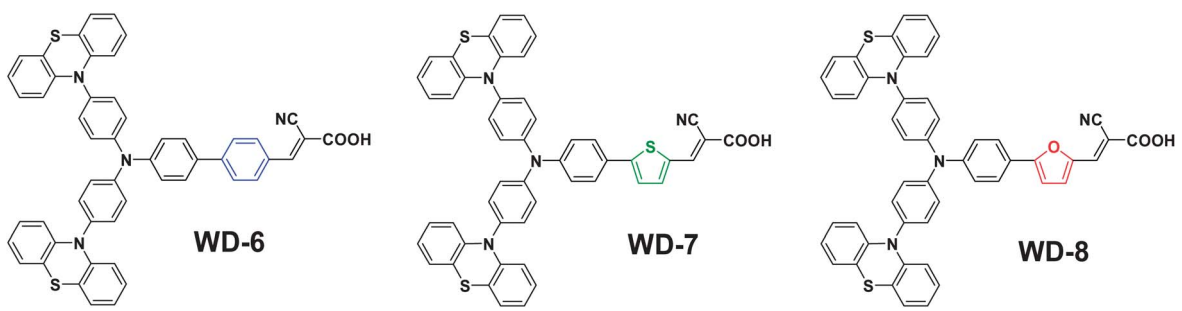

Scheme 1 Molecular structures of the organic dyes in this study.

equipped with a 500 W xenon lamp (Aosiyuan Technology & Science Co., Ltd, China) were used for photocurrent action spectrum measurements. Electrochemical impedance spectroscopy (EIS) data were obtained by using a Solartron 1255B frequency analyzer and a Solartron SI 1287 electrochemical interface system.

Synthesis

***N*-(4-(10*H*-Phenothiazin-10-yl)phenyl)-*N*-(4-iodophenyl)-4-(10*H*-phenothiazin-10-yl)benzenamine (1).** Tris(4-iodophenyl) amine (2.0 g, 3.2 mmol), phenothiazine (1.91 g, 9.6 mmol), potassium carbonate (3.18 g, 23.0 mmol), activated copper bronze (0.83 g, 13.0 mmol) and 18-crown-6 (0.10 g, 0.38 mmol) were refluxed in 1,2-dichlorobenzene (30 ml) for 36 h. The solvent was removed by decompressing distillation and the residue was purified by column chromatography on silica gel using dichloromethane and petroleum ether (60–90 °C) in the ratio of 1 : 2 (v/v) as the eluent to give **1** as a white solid (0.35 g, yield 14.5%). ^{1}H-NMR (400 MHz, DMSO-d_6) δ: 7.731 (d, $J = 8.4$ Hz, 2H), 7.362 (s, 8H), 7.081 (d, $J = 8.4$ Hz, 2H), 7.062 (d, $J = 8.4$ Hz, 4H), 6.980–6.931 (m, 4H), 6.858–6.807 (m, 4H), 6.331 (d, $J =$ 8.4 Hz, 4H). HRMS (ESI, *m*/*z*): $[M + H]^+$ calcd for ($C_{42}H_{28}IN_3S_2$): 766.0769; found: 766.0764.

5-(4-(Bis(4-(10*H*-phenothiazin-10-yl)phenyl)amino)phenyl) phenyl-2-carbaldehyde (2). Under N_2 atmosphere, a mixture of **1** (306 mg, 0.4 mmol), 4-formylphenylboronic acid (72 mg, 0.48 mmol), $Pd(PPh_3)_4$ (14 mg, 0.0114 mmol), 2 M aqueous solution of K_2CO_3 (2 ml) in dry THF (20 ml) was refluxed overnight (Scheme 2). The reaction mixture was extracted with CH_2Cl_2, water and brine. The organic layer was dried with anhydrous $MgSO_4$ and then the solvent was removed by rotary evaporation. The residue was purified by column chromatography on silica gel using dichloromethane and petroleum ether in the ratio of 2 : 1 (v/v) as the eluent to give **2** as a yellow solid (74 mg, 25%). ^{1}H-NMR (400 MHz, DMSO-d_6) δ: 10.046 (s, 1H), 7.995 (d, $J = 8.0$ Hz, 2H), 7.938 (d, $J = 8.4$ Hz, 2H), 7.851 (d, $J = 8.8$ Hz, 2H), 7.409–7.370 (m, 10H), 7.099–7.081 (m, 4H), 7.010 (t, $J = 7.6$ Hz, 4H), 6.890 (t, $J = 7.6$ Hz, 4H), 6.369 (d, $J = 7.6$ Hz, 4H). HRMS (ESI, *m*/*z*): $[M + H]^+$ calcd for ($C_{49}H_{33}N_3OS_2$): 744.2065; found: 744.1808.

5-(4-(Bis(4-(10*H*-phenothiazin-10-yl)phenyl)amino)phenyl) thiophene-2-carbaldehyde (3). A procedure similar to that for compound **2** but with 5-formyl-2-thiopheneboronic acid (75 mg, 0.48 mmol) instead of 4-formylphenylboronic acid. Yield: 27%. ^{1}H-NMR (400 MHz, DMSO-d_6) δ: 9.895 (s, 1H), 8.045 (d, $J = 4$ Hz, 1H), 7.855–7.833 (m, 2H), 7.697 (d, $J = 4$ Hz, 1H), 7.415 (d, $J = 2.4$ Hz, 8H), 7.316 (d, $J = 8.8$ Hz, 2H), 7.109–7.086 (dd, $J =$ 1.6 Hz, 4H), 7.034–6.991 (td, $J = 1.6$ Hz, 4H), 6.915–6.875 (td, $J = 1.2$ Hz, 4H), 6.373 (d, $J = 8.4$ Hz, 4H). HRMS (ESI, *m*/*z*): $[M + H]^+$ calcd for ($C_{47}H_{31}N_3OS_3$): 750.1629; found: 750.1716.

5-(4-(Bis(4-(10*H*-phenothiazin-10-yl)phenyl)amino)phenyl) furan-2-carbaldehyde (4). A procedure similar to that for compound **2** but with 5-formyl-2-furanboronic acid (67 mg, 0.48 mmol) instead of 4-formylphenylboronic acid. Yield: 25%. ^{1}H-NMR (400 MHz, DMSO-d_6) δ: 9.580 (s, 1H), 7.894 (d, $J = 8.4$ Hz, 2H), 7.665 (d, $J = 3.6$ Hz, 1H), 7.413 (s, 8H), 7.338 (d, $J = 8.8$ Hz, 2H), 7.214 (d, $J = 4$ Hz, 1H), 7.098 (d, $J = 7.6$ Hz, 4H), 7.013 (t, $J = 8$ Hz, 4H), 6.895 (t, $J = 7.6$ Hz, 4H), 6.378 (d, $J = 7.6$ Hz, 4H). HRMS (ESI, *m*/*z*): $[M + H]^+$ calcd for ($C_{47}H_{31}N_3O_2S_2$): 734.1858; found: 734.1790.

(*E*)-3-(5-(4-(Bis(4-(10*H*-phenothiazin-10-yl)phenyl)amino) phenyl)benzene-2-yl)-2-cyanoacrylic acid (WD-6). A CH_3CN (10 ml) solution of **2** (186 mg, 0.25 mmol), 2-cyanoacetic acid (43 mg, 0.5 mmol) and a few drops of piperidine was charged sequentially in a three-necked flask and heated to reflux for 10 h. After cooling to room temperature, solvents were removed by rotary evaporation, and the residue was purified by silica gel column chromatography with CH_2Cl_2 : CH_3OH (10 : 1, v/v) as eluent to afford the dye **WD-6** as a dark red solid (132 mg, yield 65%). ^{1}H-NMR (400 MHz, DMSO-d_6) δ: 8.365 (s, 1H), 8.145 (d, $J = 8.8$ Hz, 2H), 7.932 (d, $J = 8.4$ Hz, 2H), 7.868 (d, $J = 8.8$ Hz, 2H), 7.432–7.359 (m, 10H), 7.098–7.076 (dd, $J = 1.2$ Hz, 4H), 7.028–6.985 (m, 4H), 6.906–6.866 (td, $J = 0.8$ Hz, 4H), 6.368 (d, $J = 7.6$ Hz, 4H). HRMS (ESI, *m*/*z*): $[M + H]^+$ calcd for ($C_{52}H_{34}N_4O_2S_2$): 811.2123; found: 811.2135.

(*E*)-3-(5-(4-(Bis(4-(10*H*-phenothiazin-10-yl)phenyl)amino) phenyl)thiophen-2-yl)-2-cyanoacrylic acid (WD-7). A procedure similar to that for the dye **WD-6** but with compound **3** (187 mg, 0.25 mmol) instead of compound **2**. The dye **WD-7** as dark red solid (122 mg, yield 60%). ^{1}H-NMR (400 MHz, DMSO-d_6) δ: 8.492 (s, 1H), 8.023 (d, $J = 4.4$ Hz, 1H), 7.821 (d, $J = 8.4$ Hz, 2H), 7.711 (d, $J = 4$ Hz, 1H), 7.442–7.386 (m, 8H), 7.310 (d, $J = 8.4$ Hz, 2H), 7.103–7.080 (dd, $J = 1.6$ Hz, 4H), 7.029–6.986 (td, $J =$ 1.6 Hz, 4H), 6.910–6.870 (td, $J = 1.2$ Hz, 4H), 6.372 (d, $J = 8$ Hz, 4H). HRMS (ESI, *m*/*z*): $[M + H]^+$ calcd for ($C_{50}H_{32}N_4O_2S_3$): 817.1687; found: 817.1785.

(*E*)-3-(5-(4-(Bis(4-(10*H*-phenothiazin-10-yl)phenyl)amino) phenyl)furan-2-yl)-2-cyanoacrylic acid (WD-8). A procedure similar to that for the dye **WD-6** but with compound **4** (184 mg, 0.25 mmol) instead of compound **2**. The dye **WD-8** as dark red solid (128 mg, yield 64%). ^{1}H-NMR (400 MHz, DMSO-d_6) δ: 8.048 (s, 1H), 7.929 (d, $J = 8.8$ Hz, 2H), 7.556 (d, $J = 3.6$ Hz, 1H), 7.433–7.379 (m, 8H), 7.356 (d, $J = 0.8$ Hz, 2H), 7.292 (d, $J = 4$ Hz, 1H), 7.097–7.075 (dd, $J = 1.6$ Hz, 4H), 7.027–6.984 (m, 4H), 6.904–6.864 (td, $J = 0.8$ Hz, 4H), 6.380 (d, $J = 8$ Hz, 4H). HRMS (ESI, *m*/*z*): $[M - H]^+$ calcd for ($C_{50}H_{32}N_4O_3S_2$): 799.1916; found: 799.1956.

Results and discussion

Absorption properties in solution and on TiO_2 films

Fig. 1 shows the UV-vis spectra of the three organic dyes, **WD-6**, **WD-7**, and **WD-8**, measured in acetonitrile solution. The corresponding spectroscopic parameters extracted are summarized in Table 1. Each of these organic dyes exhibited two major absorption bands at 280–360 nm and 360–550 nm. The short wavelength bands were assigned to the localized aromatic π–π* transitions, and the long wavelength ones to intramolecular charge-transfer (ICT) transitions. The intensity of π–π* transitions is higher than that of the ICT transitions. The absorption

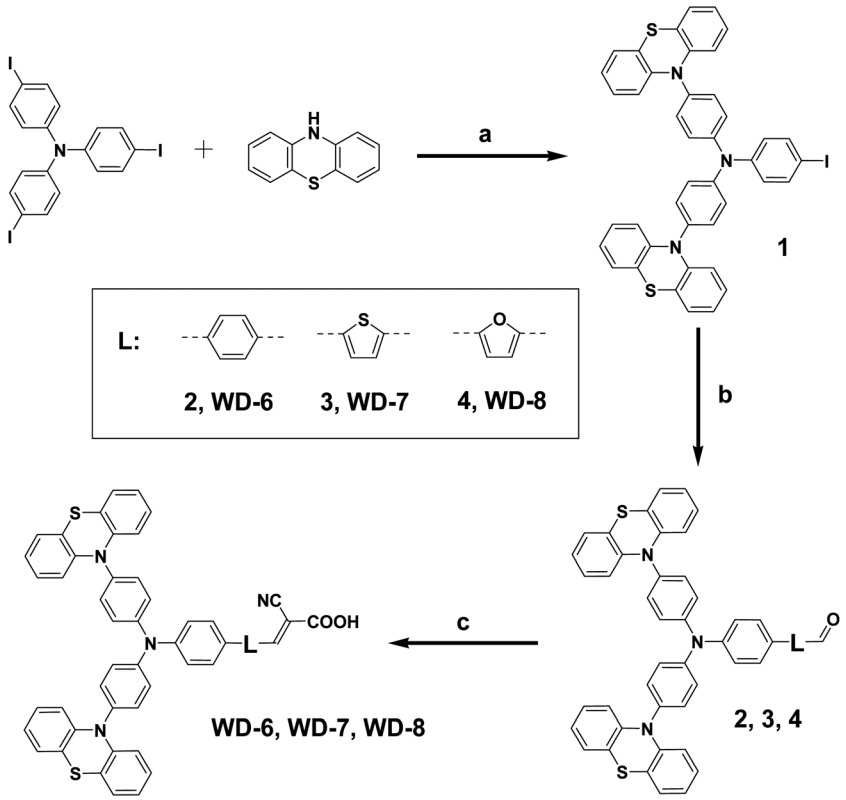

Scheme 2 The synthetic procedure of the target organic dyes. Reagents: (a) phenothiazine, 1,2-dichlorobenzene, Cu, K_2CO_3, 18-crown-6; (b) 4-formylphenylboronic acid (or 5-formyl-2-thiopheneboronic acid, or 5-formyl-2-furanboronic acid), $Pd(PPh_3)_4$, K_2CO_3, THF; (c) 2-cyanoacetic acid, piperidine, acetonitrile.

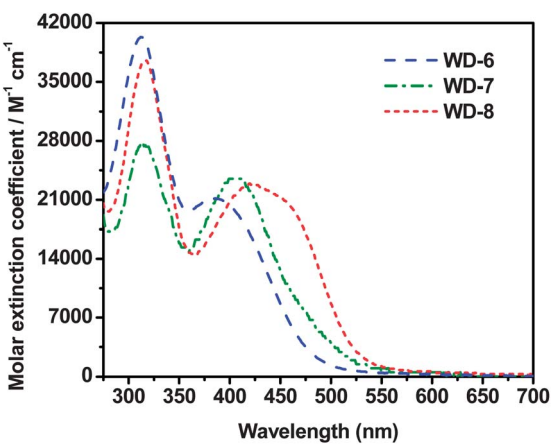

Fig. 1 Absorption spectra of the three dyes in acetonitrile.

maxima (λ_{max}) of **WD-6–8** in the long wavelength region were at 385, 406, and 421 nm, respectively. The λ_{max} of **WD-7** (thiophene linker) and **WD-8** (furan linker) was red-shifted 33 nm and 38 nm compared with that of **WD-6** with the benzene linker. This was due to better delocalization of electrons over the whole molecule when thiophene or furan was used as the conjugated linker rather than benzene. The molar extinction coefficients at λ_{max} for **WD-6–8** were 21 100, 23 580, and 22 890 M^{-1} cm^{-1}, respectively. It is known that a wider absorption range is favorable to the performance of DSSCs, as more photons can be harvested. According to the λ_{max} and molar extinction coefficients of these organic dyes, it is clear that **WD-7** and **WD-8** have a better ability to harvest light than **WD-6**, which would lead to a higher photocurrent for organic dyes **WD-7** and **WD-8**.

Fig. 2 shows the absorption spectra of the three dyes on 3 μm thick TiO_2 films after 12 h adsorption. Compared to the

Table 1 UV-vis and electrochemical data of the three dyes

Dye	λ_{max}[a]/nm (ε[b]/M^{-1} cm^{-1})	λ_{max}[c]/nm	E_{ox}[d]/V (*vs* NHE)	E_{0-0}[e]/eV	E_{red}[f]/V (*vs.* NHE)
WD-6	385 (21 100)	385	1.28	2.34	−1.06
WD-7	406 (23 580)	418	1.21	2.25	−1.04
WD-8	421 (22 890)	423	1.14	2.19	−1.05

[a] Absorption spectra were measured in acetonitrile (2.5×10^{-5} M). [b] The molar extinction coefficient at λ_{max} of the absorption spectra. [c] Absorption maximum on TiO_2 film. [d] E_{ox} was measured in CH_2Cl_2 with 0.1 M n-Bu_4NPF_6 as electrolyte (scanning rate: 100 mV s^{-1}, working electrode and counter electrode: Pt wires, and reference electrode: Ag/AgCl), potentials measured *vs* Ag/AgCl were converted to normal hydrogen electrode (NHE) by addition of +0.2 V. [e] E_{0-0} values were calculated from the absorption spectral onsets of these dyes.[9c,f] E_{red} was calculated from $E_{ox} - E_{0-0}$.

spectrum in acetonitrile solution, the sharp shift of absorption peaks for **WD-6–8** on TiO_2 films has not been observed (Table 1). As illustrated with **WD-8**, the ICT absorption peak is slightly red-shifted by only 2 nm from 421 nm in solution to 423 nm on 3 μm TiO_2 film. This may be ascribed to the starburst 2D structure, which prevented the strong tendency for the dyes to aggregate on the TiO_2 film, to a large degree. This method for the prevention of aggregation might be better than the usage of the coabsorption of the dyes with deoxycholic acid, which was also able to prevent aggregation and hence improve the photovoltaic performance by means of improving both photocurrent and photovoltage, but unavoidably and significantly decreased dye adsorption and limited the photovoltaic performance. It is confirmed that this is an effective way to lower the tendency to aggregate by introducing phenothiazine groups as additional electron donors into the triphenylamine donor.

Electrochemical properties

To evaluate the possibility of electron transfer between the TiO_2/dye/redox electrolyte systems, cyclic voltammetry (CV) was performed in CH_2Cl_2 solution, using 0.1 M tetrabutylammonium hexafluorophosphate as the supporting electrolyte (Fig. 3). The oxidation potential of the organic dyes was determined from the peak potentials by CV, the oxidation potential *vs.* NHE (E_{ox}) corresponds to the highest occupied molecular orbital (HOMO), while the lowest unoccupied molecular orbital (LUMO), could be calculated from $E_{ox} - E_{0\text{-}0}$.[19] As shown in Table 1 and Fig. 4, the HOMO levels are more positive than the iodine/iodide redox potential value (0.4 V *vs.* NHE), indicating that the oxidized dye molecules formed after electron injection into the conduction band of TiO_2 could be regenerated by the reducing species in the electrolyte solution. The LUMO levels of the dyes are sufficiently more negative than the CB level of the TiO_2 electrode (−0.5 V *vs.* NHE), which implies that electron injection from the excited dye into the conduction band of TiO_2 is energetically permitted. Therefore, these organic dyes could be used as good sensitizers in DSSCs. The schematic energy levels of the dyes based on absorption and electrochemical data are shown in Fig. 4.

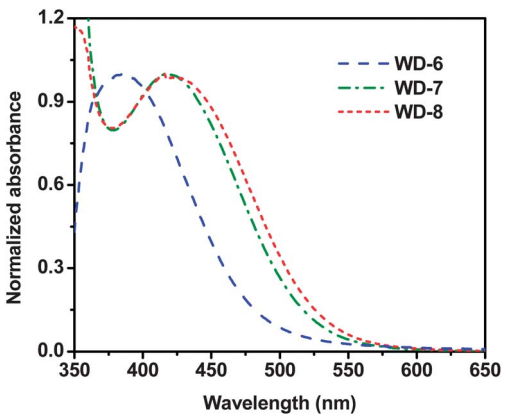

Fig. 2 Absorption spectra of TiO_2 electrodes sensitized by the three dyes.

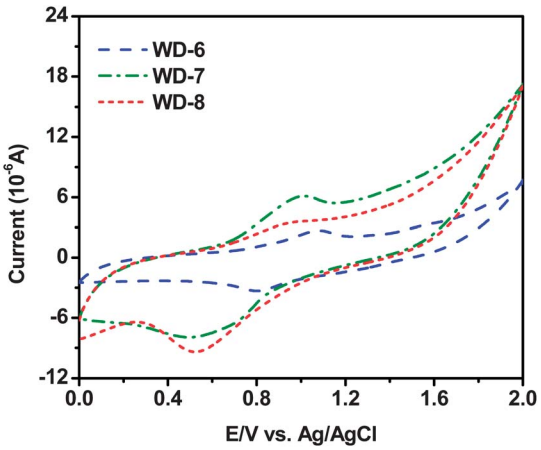

Fig. 3 Cyclic voltammograms of the three dyes.

Theoretical calculations

To gain insight into the molecular structures and electron distribution, the geometries of the dyes were optimized by density functional theory calculations at the B3LYP/6-31G level with Gaussian 03.[20] As shown in Fig. 5, for the three organic dyes, HOMO-1/HOMO are only localized on a phenothiazine ring, and HOMO-2 is distributed along the triphenylamine and linker system. The LUMO of the three dyes is delocalized across the linker and acceptor system. It may imply that the nonplanar phenothiazine blocked by triphenylamine can make electron distribution of HOMO-1 and HOMO separate from electron distribution of LUMO. The well-overlapped HOMO-2 and LUMO orbitals on the linker unit suggest the well inductive or withdrawing electron tendency from triphenylamine donor unit to the cyanoacetic acid unit. Thus, the HOMO-2 → LUMO excitation induced by light irradiation could move the excited electron distribution from the triphenylamine unit to the cyanoacetic acid unit, and injected into the conduction band of TiO_2 through the anchoring group. The electronic transition in the visible band with the largest oscillator strength was found to correspond to the excitation of HOMO-2 to LUMO (the oscillator strengths of HOMO-1 → LUMO and HOMO → LUMO transitions are almost zero).[21]

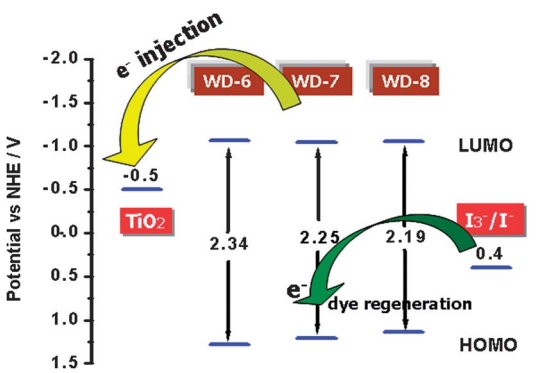

Fig. 4 Schematic energy levels of the three dyes based on absorption and electrochemical data.

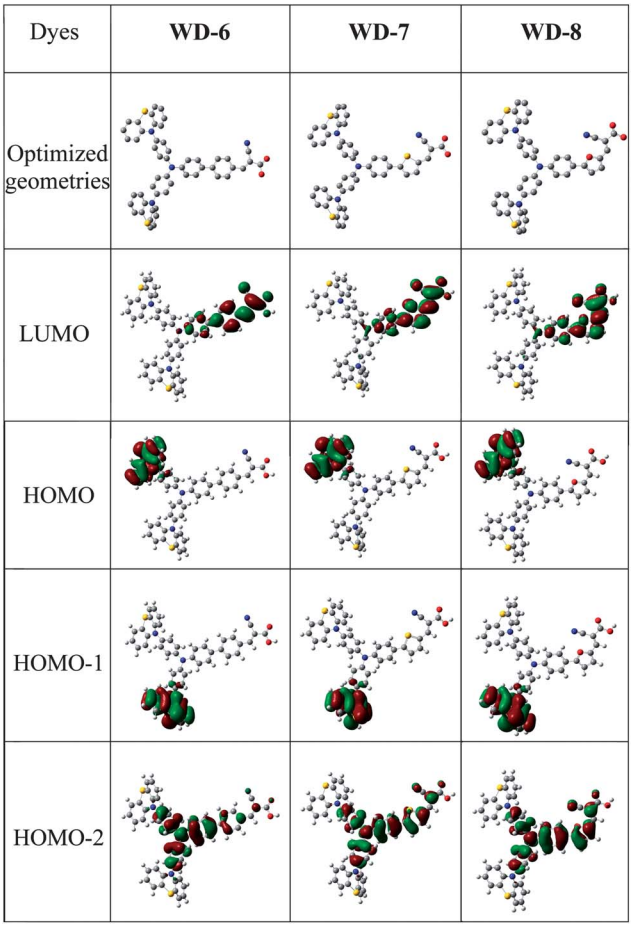

Fig. 5 Frontier orbitals of the three dyes optimized at the B3LYP/6-31G level.

Photovoltaic performances of DSSCs

Fig. 6 shows the incident photon-to-current efficiency (IPCE) data as a function of the wavelength for DSSCs based on the organic dyes **WD-6**, **WD-7** and **WD-8**.

All three organic dyes could efficiently convert the light to photocurrents in the region from 400 to 650 nm. The IPCE spectra changing tendency of the organic dyes are in accordance with their UV-vis absorption spectra on the TiO_2 film. However, the onsets of the IPCE spectra for **WD-6**, **WD-7** and **WD-8** are 655, 665 and 675 nm, respectively, which are significantly broadened compared with those of their UV-vis absorption spectra on the TiO_2 film. The IPCE values of DSSCs based on **WD-7** and **WD-8** exceeded 60% from 400 nm to 535 nm (with the highest value of 79.1% at 470 nm) and from 400 to 547 nm (with the highest value of 79.2% at 475 nm), respectively. In the DSSC based on **WD-6**, the IPCE values relatively exceed 60% from 408 nm to 493 nm (with the highest value of 69.1% at 445 nm). The IPCE of **WD-8** is higher and broader than those of **WD-6** and **WD-7** in the region from 470 nm to 650 nm, indicating that the **WD-8** sensitized TiO_2 electrode would generate the higher conversion efficiency among the three dyes.

The photocurrent-density–photovoltage (J–V) curves of the DSSCs based on **WD-6**, **WD-7** and **WD-8** performed under simulated AM 1.5 solar irradiation (100 mW cm^{-2}) are shown in Fig. 7. The photovoltaic properties of these dye-based DSSCs are summarized in Table 2. The solar cell based on **WD-6** shows an efficiency of 4.90%, with a short-circuit photocurrent density (J_{sc}) of 10.86 mA cm^{-2}, an open-circuit photovoltage (V_{oc}) of 635 mV, and a fill factor (ff) of 0.71. When we replaced the benzene unit with a thiophene unit to construct **WD-7**, the performance of the solar cell based on **WD-7** improved (η = 6.02%, J_{sc} = 12.64 mA cm^{-2}, V_{oc} = 680 mV, and ff = 0.70). Afterwards, when we replaced the thiophene unit in **WD-7** with a furan unit to construct **WD-8**, a further increase in performance of the solar cell based on **WD-8** was achieved (η = 6.79%, J_{sc} = 14.43 mA cm^{-2}, V_{oc} = 682 mV, and ff = 0.69). Under the same measurement conditions, the solar cell based on dye **N3** generated an efficiency of 8.05% (J_{sc} = 17.55 mA cm^{-2}, V_{oc} = 685 mV, and ff = 0.67).

According to Fig. 7 and Table 2, it is clear that the photovoltaic performances of the DSSCs can be affected by the different conjugated linkers in the starburst 2D–π–A organic dyes. In comparison with **WD-6**, the J_{sc} and V_{oc} values of **WD-7** and **WD-8** are improved by introducing a thiophene and a furan linker, respectively. **WD-7** and **WD-8** have the higher J_{sc}, which might be due to the higher light harvesting efficiency than that of **WD-6**. Clearly, the DSSCs based on **WD-7** and **WD-8** possessed higher V_{oc}. The higher J_{sc} and V_{oc} for the DSSCs of **WD-7** and **WD-8** lead to the higher efficiencies finally.

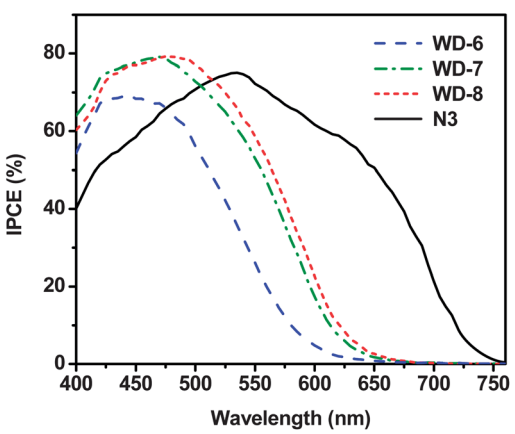

Fig. 6 IPCE spectra of DSSCs with the three dyes.

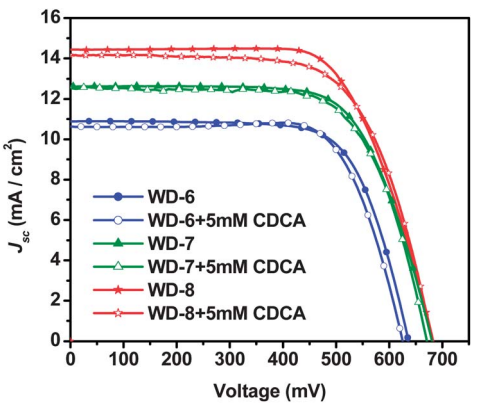

Fig. 7 J–V characteristics measured at an irradiation of 100 mW cm^{-2} simulated AM1.5 sunlight.

Table 2 Photovoltaic performances of DSSCs based on the three dyes

Dye	CDCA/mM	J_{sc}/mA cm^{-2}	V_{oc}/mV	ff	η (%)	τ_e/ms
WD-6	0	10.86	635	0.71	4.90	39.91
	5	10.63	625	0.73	4.85	
WD-7	0	12.64	680	0.70	6.02	56.47
	5	12.53	671	0.70	5.89	
WD-8	0	14.43	682	0.69	6.79	63.19
	5	14.17	681	0.67	6.47	

In order to further probe the behavior of these organic dyes on the surface of TiO_2, the function of co-adsorbents was investigated. Chenodeoxycholic acid (CDCA) is the most popular co-adsorbent, which binds strongly to the surface of nanostructured TiO_2, being able to displace dye molecules from the semiconductor surface and therefore hindering the formation of sensitizer aggregates.[22] Thus, the performances of the DSSCs in the presence of CDCA were studied. The results were collected in Table 2, and the corresponding J–V curves are shown in Fig. 7. It was found that the J_{sc} of the solar cells based on these dyes and CDCA decreased. CDCA did not improve the corresponding device's performance, however, it decreased the power conversion efficiency. A possible explanation is that the amount of dye adsorbed on the TiO_2 surface was reduced by the coadsorption of CDCA, resulting in a loss of active light harvesting, indicating that CDCA was not necessary for these dyes to improve their performance. In addition, the V_{oc} values of the DSSCs in the presence of CDCA were decreased; this is because adsorption of CDCA leaves protons on the TiO_2 surface and, hence, charges the surface positively shifted by the coadsorption of CDCA, resulting in V_{oc} loss.[23] These results could be considered as a hint that these dyes with a starburst 2D–π–A structure nearly did not aggregate on the TiO_2 surface.

To further elucidate the photovoltaic results and obtain more interfacial charge transfer information in DSSCs sensitized by **WD-6**, **WD-7** and **WD-8**, electrochemical impedance spectroscopy (EIS) was also performed in the dark under a forward bias of −0.65 V.[24] The Nyquist and Bode plots for **WD-6**, **WD-7** and **WD-8** sensitized cells are shown in Fig. 8a and b, respectively. Nyquist plots have two semicircles and the larger semicircle indicates charge recombination resistance at the TiO_2/dye/electrolyte interface. As can be seen from Fig. 8a that the radius of the larger semicircle increases in the order of **WD-8** > **WD-7** > **WD-6**, indicating that the charge recombination resistance is increased in the order **WD-6** > **WD-7** > **WD-8**. This is to some extent consistent with the order of decreasing V_{oc}: **WD-8** (682 mV) > **WD-7** (680 mV) > **WD-6** (635 mV).

In the Bode phase plots (Fig. 8b), the lower-frequency peak is indicative of the charge-transfer process of injected electrons in TiO_2. The higher V_{oc} of **WD-7** and **WD-8** can be further explained by electron lifetime, calculated through the relation $\tau_e = 1/(2\pi f)$ (f is the peak frequency of lower-frequency range in EIS Bode plot). For the three devices, the peak frequency of lower-frequency range decreased in the order of **WD-6** > **WD-7** > **WD-8**, and the electron lifetime was enhanced in reverse with the calculated values of 39.91, 56.47, and 63.19 ms, respectively. Thus, **WD-8** has the longest electron lifetime, indicative of a more effective suppression of the back reaction between the injected electrons and the electrolyte, resulting in the improvement of the V_{oc} due to reduced charge recombination rate. The combination of the highest V_{oc} and J_{sc} values (*vide supra*) affords the best photovoltaic performance of the solar cell based on **WD-8**.

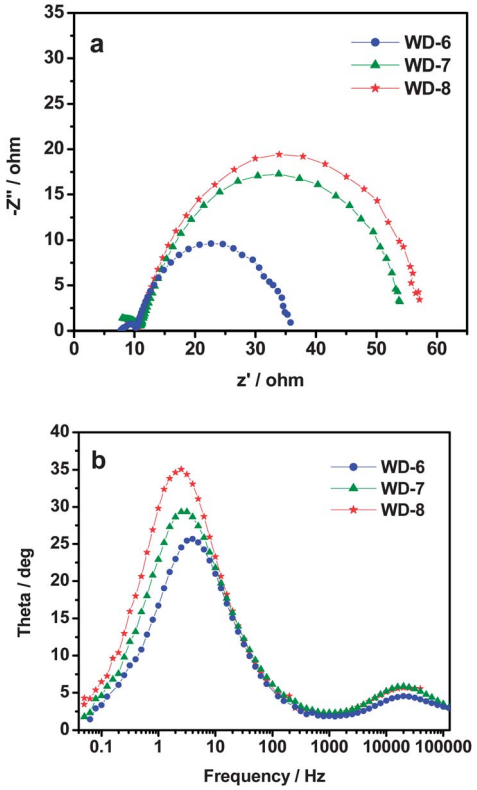

Fig. 8 EIS spectra of DSSCs based on the three dyes measured at −0.65 V forward bias in the dark: (a) Nyquist and (b) Bode phase plots.

Conclusion

In this work, two phenothiazine groups as additional electron donors were introduced into a triphenylamine unit to form a starburst 2D structure. A series of efficient organic dyes (**WD-6**, **WD-7** and **WD-8**) containing this starburst 2D structure and a 2-cyanoacetic acid acceptor linked by different π-conjugated linkers (benzene, thiophene, and furan) have been synthesized, characterized and applied in DSSCs. The phenothiazine group with a butterfly conformation in these organic dyes has an effect on preventing the molecular π–π aggregation. The DSSCs made with these organic dyes displayed remarkable overall conversion efficiency in a range of 4.90–6.79%. The best performance of a solar cell based on **WD-8** (furan group as the conjugated linker) was achieved (η = 6.79%, J_{sc} = 14.43 mA cm^{-2}, V_{oc} = 682 mV, and ff = 0.69). The DSSCs based on **WD-7** and **WD-8** have higher V_{oc} and J_{sc} values than those of **WD-6** because of their more efficient dark current suppression and light harvesting. According to the EIS analysis, both the resistance for charge recombination and the electron lifetime were increased from **WD-6** to **WD-7** and **WD-8**, indicating that the introduction of the furan unit as the linker in starburst phenothiazine–triphenylamine based organic dyes could improve photovoltaic

performance compared with the benzene and thiophene units as the linker. Coadsorption of CDCA did not improve the conversion efficiency of the devices based on the three dyes, indicating that these starburst 2D–π–A dyes nearly did not aggregate on the TiO_2 surface. The results from this work strongly indicate that the increasing of the twisted non-planar structure in organic dyes is a promising way to improve the performance in DSSCs.

Acknowledgements

We thank the National Natural Science Foundation of China (Grant nos. 20873015, 21272033), the Fundamental Research Funds for the Central Universities (Grant no. ZYGX2010J035), the Innovation Funds of State Key Laboratory of Electronic Thin Films and Integrated Device (Grant no. CXJJ201104) and Beijing National Laboratory for Molecular Sciences (BNLMS) for financial support.

Notes and references

1 B. O'Regan and M. Grätzel, *Nature*, 1991, **353**, 737.
2 M. Grätzel, *Acc. Chem. Res.*, 2009, **42**, 1788.
3 (*a*) L. Y. Han, A. Islam, H. Chen, C. Malapaka, B. Chiranjeevi, S. F. Zhang, X. D. Yang and M. Yanagida, *Energy Environ. Sci.*, 2012, **5**, 6507; (*b*) M. Chandrasekharam, B. Chiranjeevi, K. S. V. Gupta, S. P. Singh, A. Islam, L. Y. Han and M. L. Kantam, *J. Nanosci. Nanotechnol.*, 2012, **12**, 4489.
4 Y. C. Chang, C. L. Wang, T. Y. Pan, S. H. Hong, C. M. Lan, H. H. Kuo, C. F. Lo, H. Y. Hsu, C. Y. Lin and E. W. G. Diau, *Chem. Commun.*, 2011, **47**, 8910.
5 A. Yella, H. W. Lee, H. N. Tsao, C. Yi, A. K. Chandiran, M. K. Nazeeruddin, E. W. G. Diau, C. Y. Yeh, S. M. Zakeeruddin and M. Grätzel, *Science*, 2011, **334**, 629.
6 (*a*) K. Hara, K. Sayama, Y. Ohga, A. Shinpo, S. Suga and H. Arakawa, *Chem. Commun.*, 2001, 569; (*b*) K. D. Seo, I. T. Choi, Y. G. Park, S. Kang, J. Y. Lee and H. K. Kim, *Dyes Pigm.*, 2012, **94**, 469; (*c*) S. Agrawal, P. Dev, N. J. English, K. R. Thampi and J. M. D. MacElroy, *J. Mater. Chem.*, 2011, **21**, 11101.
7 (*a*) L. Etgar, J. H. Park, C. Barolo, V. Lesnyak, S. K. Panda, P. Quagliotto, S. G. Hickey, M. K. Nazeeruddin, A. Eychmuller, G. Viscardi and M. Grätzel, *RSC Adv.*, 2012, **2**, 2748; (*b*) K. Funabiki, H. Mase, Y. Saito, A. Otsuka, A. Hibino, N. Tanaka, H. Miura, Y. Himori, T. Yoshida, Y. Kubota and M. Matsui, *Org. Lett.*, 2012, **14**, 1246.
8 (*a*) B. Liu, Q. B. Liu, D. You, X. Y. Li, Y. Naruta and W. H. Zhu, *J. Mater. Chem.*, 2012, **22**, 13348; (*b*) U. M. Tefashe, M. Rudolph, H. Miura, D. Schlettwein and G. Wittstock, *Phys. Chem. Chem. Phys.*, 2012, **14**, 7533; (*c*) S. Higashijima, Y. Inoue, H. Miura, Y. Kubota, K. Funabiki, T. Yoshida and M. Matsui, *RSC Adv.*, 2012, **2**, 2721.
9 (*a*) W. J. Wu, J. B. Yang, J. L. Hua, J. Tang, L. Zhang, Y. T. Long and H. Tian, *J. Mater. Chem.*, 2010, **20**, 1772; (*b*) Z. Q. Wan, C. Y. Jia, J. Q. Zhang, Y. D. Duan, Y. Lin and Y. Shi, *J. Power Sources*, 2012, **199**, 426; (*c*) M. Marszalek, S. Nagane, A. Ichake, R. Humphry-Baker, V. Paul, S. M. Zakeeruddin and M. Grätzel, *J. Mater. Chem.*, 2012, **22**, 889; (*d*) M. H. Tsao, T. Y. Wu, H. P. Wang, I. W. Sun, S. G. Su, Y. C. Lin and C. W. Chang, *Mater. Lett.*, 2011, **65**, 583.
10 (*a*) S. Haid, M. Marszalek, A. Mishra, M. Wielopolski, J. Teuscher, J. E. Moser, R. Humphry-Baker, S. M. Zakeeruddin, M. Grätzel and P. Baeuerle, *Adv. Funct. Mater.*, 2012, **22**, 1291; (*b*) M. F. Xu, M. Zhang, M. Pastore, R. Z. Li, F. De Angelis and P. Wang, Peng, *Chem. Sci.*, 2012, **3**, 976; (*c*) K. Pei, Y. Z. Wu, W. J. Wu, Q. Zhang, B. Q. Chen, H. Tian and W. H. Zhu, *Chem.–Eur. J.*, 2012, **18**, 8190.
11 (*a*) S. Kim, J. K. Lee, S. O. Kang, J. Ko, J. H. Yum, S. Fantacci, F. D. Angelis, D. D. Censo, M. K. Nazeeruddin and M. Grätzel, *J. Am. Chem. Soc.*, 2006, **128**, 16701; (*b*) S. Ko, H. Choi, M. S. Kang, H. Hwang, H. Ji, J. Kim, J. Ko and Y. Kang, *J. Mater. Chem.*, 2010, **20**, 2391; (*c*) S. Higashijima, Y. Inoue, H. Miura, Y. Kubota, K. Funabiki, T. Yoshida and M. Matsui, *RSC Adv.*, 2012, **2**, 2721.
12 (*a*) K. Hara, Z. S. Wang, Y. Cui, A. Furube and N. Koumura, *Energy Environ. Sci.*, 2009, **2**, 1109; (*b*) C. J. Chen, J. Y. Liao, Z. G. Chi, B. J. Xu, X. Q. Zhang, D. B. Kuang, Y. Zhang, S. W. Liu and J. R. Xu, *J. Mater. Chem.*, 2012, **22**, 8994; (*c*) H. Lai, J. Hong, P. Liu, C. Yuan, Y. X. Li and Q. Fang, *RSC Adv.*, 2012, **2**, 2427.
13 Y. Hao, X. C. Yang, J. Y. Cong, A. Hagfeldt and L. C. Sun, *Tetrahedron*, 2012, **68**, 552.
14 J. Tang, W. J. Wu, J. L. Hua, J. Li and H. Tian, *Energy Environ. Sci.*, 2009, **2**, 982.
15 (*a*) J. Tang, J. L. Hua, W. J. Wu, J. Li, Z. G. Jin, Y. T. Long and H. Tian, *Energy Environ. Sci.*, 2010, **3**, 1736; (*b*) C. Teng, X. C. Yang, S. F. Li, M. Cheng, A. Hagfeldt, L. Z. Wu and L. C. Sun, *Chem. Eur. J.*, 2010, **16**, 13127; (*c*) L. Alibabaei, J. H. Kim, M. Wang, N. Pootrakulchote, J. Teuscher, D. Di Censo, R. Humphry-Baker, J.-E. Moser, Y.-J. Yu, K.-Y. Kay, S. M. Zakeeruddin and M. Grätzel, *Energy Environ. Sci.*, 2010, **3**, 1757.
16 Z. Q. Wan, C. Y. Jia, Y. D. Duan, L. L. Zhou, J. Q. Zhang, Y. Lin and Y. Shi, *RSC Adv.*, 2012, **2**, 4507.
17 P. Bonhôte, A. P. Dias, N. Papageorgiou, K. Kalyanasunda-ram and M. Grätzel, *Inorg. Chem.*, 1996, **35**, 1168.
18 J. Liu, H. T. Yang, W. W. Tan, X. W. Zhou and Y. Lin, *Electrochim. Acta*, 2010, **56**, 396.
19 J. Shi, J. N. Chen, Z. F. Chai, H. Wang, R. L. Tang, K. Fan, M. Wu, H. W. Han, J. G. Qin, T. Y. Peng, Q. Q. Li and Z. Li, *J. Mater. Chem.*, 2012, **22**, 18830.
20 M. J. Frisch, G. W. Trucks, H. B. Schlegel, G. E. Scuseria, M. A. Robb, J. R. Cheeseman, J. A. Montgomery Jr, T. Vreven, K. N. Kudin, J. C. Burant, J. M. Millam, S. S. Iyengar, J. Tomasi, V. Barone, B. Mennucci, M. Cossi, G. Scalmani, N. Rega, G. A. Petersson, H. Nakatsuji, M. Hada, M. Ehara, K. Toyota, R. Fukuda, J. Hasegawa, M. Ishida, T. Nakajima, Y. Honda, O. Kitao, H. Nakai, M. Klene, X. Li, J. E. Knox, H. P. Hratchian, J. B. Cross, V. Bakken, C. Adamo, J. Jaramillo, R. Gomperts, R. E. Stratmann, O. Yazyev, A. J. Austin, R. Cammi, C. Pomelli, J. W. Ochterski, P. Y. Ayala, K. Morokuma, G. A. Voth, P. Salvador, J. J. Dannenberg, V. G. Zakrzewski, S. Dapprich, A. D. Daniels, M. C. Strain, O. Farkas, D. K. Malick, A. D. Rabuck, K. Raghavachari, J. B. Foresman, J. V. Ortiz, Q. Cui, A. G. Baboul, S. Clifford, J. Cioslowski, B. B. Stefanov, G. Liu, A. Liashenko, P. Piskorz, I. Komaromi, R. L. Martin, D. J. Fox, T. Keith, M. A. Al-Laham, C. Y. Peng, A. Nanayakkara, M. Challacombe, P. M. W. Gill, B. Johnson, W. Chen, M. W. Wong, C. Gonzalez and J. A. Pople, *Gaussian 03, Revision B.05*, Gaussian, Inc., Wallingford, CT, 2004.
21 J. B. Yang, F. L. Guo, J. L. Hua, X. Li, W. J. Wu, Y. Qu and H. Tian, *J. Mater. Chem.*, DOI: 10.1039/c2jm31929b.
22 S. Ito, H. Miura, S. Uchida, M. Takata, K. Sumioka, P. Liska, P. Comte, P. Péchy and M. Grätzel, *Chem. Commun.*, 2008, 5194.
23 N. R. Neale, N. Kopidakis, J. van de Lagemaat, M. Grätzel and A. J. Frank, *J. Phys. Chem. B*, 2005, **109**, 23183.
24 (*a*) J. Bisquert, *Phys. Chem. Chem. Phys.*, 2003, **5**, 5360; (*b*) F. Fabregat-Santiago, J. Bisquert, L. Cevey, P. Chen, M. Wang, S. M. Zakeeruddin and M. Grätzel, *J. Am. Chem. Soc.*, 2009, **131**, 558.